

Precision and dissipation of a stochastic Turing pattern

Shubhashis Rana and Andre C Barato

Department of Physics, University of Houston, Houston, Texas 77204, USA

Spontaneous pattern formation is a fundamental scientific problem that has received much attention since the seminal theoretical work of Turing on reaction-diffusion systems. In molecular biophysics, this phenomena often takes place under the influence of large fluctuations. It is then natural to inquire about the precision of such pattern. In particular, spontaneous pattern formation is a nonequilibrium phenomenon, and the relation between the precision of a pattern and the thermodynamic cost associated with it remains unexplored. Here, we analyze this relation with a paradigmatic stochastic reaction-diffusion model, the Brusselator in one spatial dimension. We find that the precision of the pattern is maximized for an intermediate thermodynamic cost, i.e., increasing the thermodynamic cost beyond this value makes the pattern less precise. Even though fluctuations get less pronounced with an increase in thermodynamic cost, we argue that larger fluctuations can also have a positive effect on the precision of the pattern.

PACS numbers: 05.70.Ln, 02.50.Ey

I. INTRODUCTION

The formation of patterns is a ubiquitous phenomenon in nature, with embryogenesis as a prominent example. In 1952, Alan Turing introduced a fundamental concept in pattern formation, he showed that a homogeneous reaction-diffusion system can form a periodic spatial profile [1]. The counter-intuitive idea introduced by Turing was that diffusion can generate an instability that leads to spontaneous pattern formation. Turing patterns have been the subject of several theoretical and experimental works [2–4].

Reaction-diffusion models that display spontaneous pattern formation are traditionally described by deterministic nonlinear partial differential equations. However, the formation of patterns often takes place in a setup where fluctuations are relevant, which requires reaction-diffusion models that take noise into account for an accurate description. For instance, the range of parameters for which a pattern is formed can be substantially increased in a stochastic reaction-diffusion model as compared to its deterministic version [5–11]. Interestingly, this concept that noise increases the region in parameter space that leads to the formation of a pattern has been recently verified in experiments [12, 13].

A different question about the formation of a pattern in a stochastic setting is: how precise is the pattern? In particular, pattern formation happens in nonequilibrium systems that dissipate energy. What is the relation between the precision of the pattern and the thermodynamic cost to maintain it? In this paper, we address these questions.

They are part of larger research program that has been carried out recently, which is the study of the relation between precision and dissipation in biophysics [14–21]. A problem in this context particularly connected with our work is the relation between the precision of temporal biochemical oscillations and energy dissipation [22–32]. Such biochemical oscillators are modeled as a system of

chemical reactions without spatial structure. Here, we analyze a system of chemical reactions with spatial structure.

We analyze the relation between precision and dissipation of a Turing pattern for a particular model, the Brusselator in one spatial dimension [7]. We consider a thermodynamically consistent version of this model which falls within the framework of stochastic thermodynamics [33]. This framework allows us to evaluate the rate of entropy production that quantifies the thermodynamic cost. It is worth mentioning that the relation between stochastic thermodynamics and deterministic reaction-diffusion models has been established in [34].

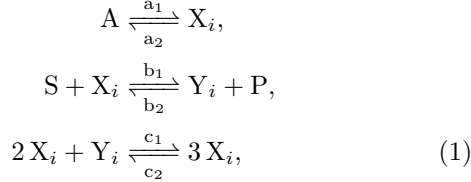
We find that increasing the thermodynamic cost does not necessarily improve the precision of a Turing pattern. There is an optimal parameter value beyond which increasing thermodynamic cost reduces the precision of the pattern. The interesting fact we explain in this paper is that fluctuations, which get less pronounced with the increase of the thermodynamic cost in our model, can have a positive effect in the precision of a Turing pattern. From a technical side, our results are obtained with numerical simulations since we consider a regime for which known analytical approximations [35] are not valid.

The paper is organized in the following way. In Sec. II we introduce the model and explain its basic phenomenology. We evaluate the rate of entropy production that quantifies the thermodynamic cost in Sec. III. In Sec. IV we define the observables that quantify the precision of a pattern and evaluate them. We conclude in Sec. V.

II. THE BRUSSELTOR IN ONE SPATIAL DIMENSION

A. Chemical reactions in a single cell

Our version of the Brusselator model in one dimension is defined in the following way. There are two chemical reactants, X and Y . The system has L cells labelled by the index $i = 1, 2, \dots, L$. In each cell, X and Y react according to the following scheme,



where the chemical species A , S and P have fixed concentrations that are sustained by chemostats. The parameters a_1 , a_2 , b_1 , b_2 , c_1 , and c_2 are transition rates. These rates already account for the dependence on the concentrations of the chemical species A , S , and P . For example, the rate b_1 is proportional to the concentration of S .

The thermodynamic force that drives the system of chemical reactions in Eq. (1) out of equilibrium is the chemical potential difference $\Delta\mu = \mu_S - \mu_P$, where μ_S (μ_P) is the chemical potential of the substrate S (product P). In order to establish a relation between $\Delta\mu$ and the transition rates we consider the following cycle with two chemical reactions: first the one with rate b_1 and then the one with rate c_1 . After this cycle, the numbers molecules X and Y remain the same, however, a molecule S is consumed and a molecule P is produced. The generalized detailed balance relation [33] is a postulate of stochastic thermodynamics that connects the thermodynamic force with transition rates. For this cycle, it reads

$$\ln \frac{b_1 c_1}{b_2 c_2} = \frac{\Delta\mu}{k_B T}, \quad (2)$$

where k_B is Boltzmann's constant and T is the temperature of the external reservoir. We set $k_B = T = 1$ throughout. If $\Delta\mu = 0$ the system fulfills detailed balance and is at equilibrium. The chemical species A cannot be consumed or produced in sequence of transition that leave the numbers of X and Y unaltered, hence, it is not related to a thermodynamic force that drives the system out of equilibrium.

B. Spatial diffusion and full model

Besides the chemical reactions in Eq. (1) the chemicals X and Y also diffuse between nearest neighbor cells. The transition from site i to site $j = i \pm 1$ is represented by

the scheme



where α and β are the diffusion rates of species X and Y , respectively. We consider periodic boundary conditions throughout, in our notation, for $i = 1$ the left nearest neighbor is $j = i - 1 = L$ and for $i = L$ the right nearest neighbor is $j = i + 1 = 1$. We point out that boundary conditions can have an important role in the formation of Turing patterns [37].

The number of X (Y) molecules in site i is denoted by n_i (m_i). The state of the system is fully specified by the vectors $\vec{n} = \{n_1, n_2, \dots, n_L\}$ and $\vec{m} = \{m_1, m_2, \dots, m_L\}$. The transition rates associated with the reactions in Eq. (1) are given by

$$\begin{aligned} T_1(n_i + 1, m_i | n_i, m_i) &= a_1, \\ T_2(n_i - 1, m_i | n_i, m_i) &= a_2 \frac{n_i}{V}, \\ T_3(n_i - 1, m_i + 1 | n_i, m_i) &= b_1 \frac{n_i}{V}, \\ T_4(n_i + 1, m_i - 1 | n_i, m_i) &= b_2 \frac{m_i}{V}, \\ T_5(n_i + 1, m_i - 1 | n_i, m_i) &= c_1 \frac{n_i^2 m_i}{V^3}, \\ T_6(n_i - 1, m_i + 1 | n_i, m_i) &= c_2 \frac{n_i}{V}, \end{aligned} \quad (4)$$

where V represents the volume of the cell. In this notation $T_\nu(n'_i, m'_i | n_i, m_i)$ is the transition rate from a configuration with n_i and m_i at site i to a configuration with n'_i, m'_i at site i . The numbers n_j and m_j for all other $j \neq i$ are the same for both configurations. The transition rates associated with the diffusion transitions represented in Eq. (3) are

$$\begin{aligned} T_7(n_i - 1, n_j + 1 | n_i, n_j) &= (\delta_{i,j-1} + \delta_{i,j+1}) \alpha \frac{n_i}{2V}, \\ T_8(m_i - 1, m_j + 1 | m_i, m_j) &= (\delta_{i,j-1} + \delta_{i,j+1}) \beta \frac{m_i}{2V}. \end{aligned} \quad (5)$$

The time evolution of the probability of a configuration (\vec{n}, \vec{m}) follows the master equation [35, 36] with the transition rates given by Eq. (4) and Eq. (5).

The parameters of the model are set to $a_1 = 1.5$, $a_2 = 1.0$, $b_2 = 0.005$, $c_1 = 1.0$, $c_2 = 0.005$, $\alpha = 1.0$, and $\beta = 20.0$. By varying the parameter b_1 we vary the thermodynamic force $\Delta\mu$ in Eq. (2). We have performed numerical simulations using the Gillespie algorithm [38]. The initial condition in our simulations is $n_i = 700$ and $m_i = 350$ for $i = 1, 2, \dots, L$. The volume V is set to $V = 500$. The system size is fixed as $L = 200$. We point out that a standard analytical method to analyze stochastic reaction-diffusion models is the linear noise approximation [35]. We resort to numerical simulations because this approximation does not work for parameter values that we are interested in, as explained below. For

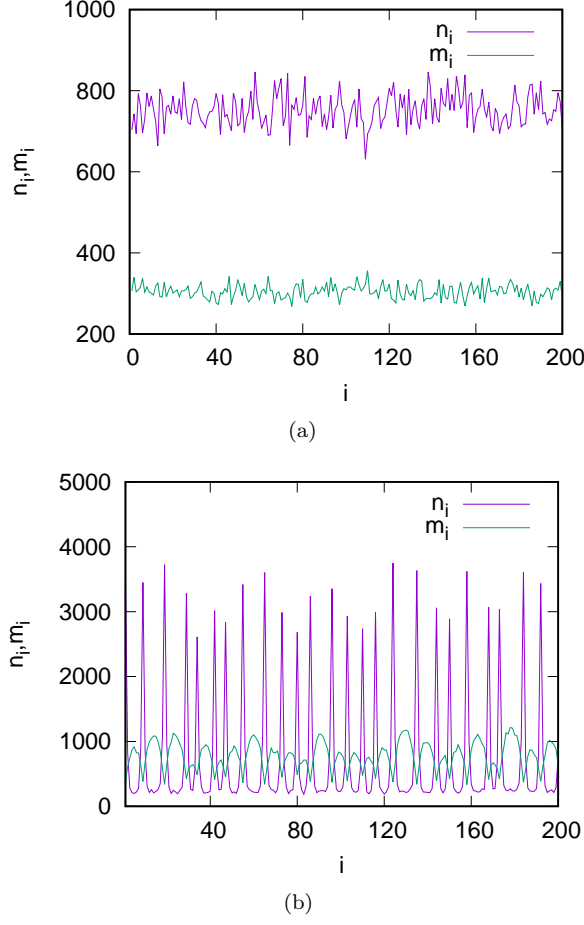


FIG. 1. (Color online) Spatial patterns. (a) Homogeneous profile $\Delta\mu = 10.5 < \Delta\mu_c$. (b) Formation of pattern for $\Delta\mu = 11.8 > \Delta\mu_c$.

the averages plotted here, we have performed 20 independent realizations. In each realization we took 50 different data points. The time interval between different data points in the same realization is 20.

C. Onset of spatial oscillations

In the limit $L \rightarrow \infty$ this model is described by deterministic equations for the average concentrations $u_i \equiv n_i/V$ and $v_i \equiv m_i/V$. These equations can be obtained with standard methods [35], and they read

$$\begin{aligned} \frac{du_i}{d\tau} &= a_1 - a_2 u_i - b_1 u_i + b_2 v_i + c_1 u_i^2 v_i - c_2 u_i^3 + \alpha \Delta u_i \\ \frac{dv_i}{d\tau} &= b_1 u_i - b_2 v_i - c_1 u_i^2 v_i + c_2 u_i^3 + \beta \Delta v_i \end{aligned} \quad (6)$$

where Δ is a discrete Laplacian operator defined as $\Delta f_i = f_{i+1} + f_{i-1} - 2f_i$. The homogeneous fixed point of the

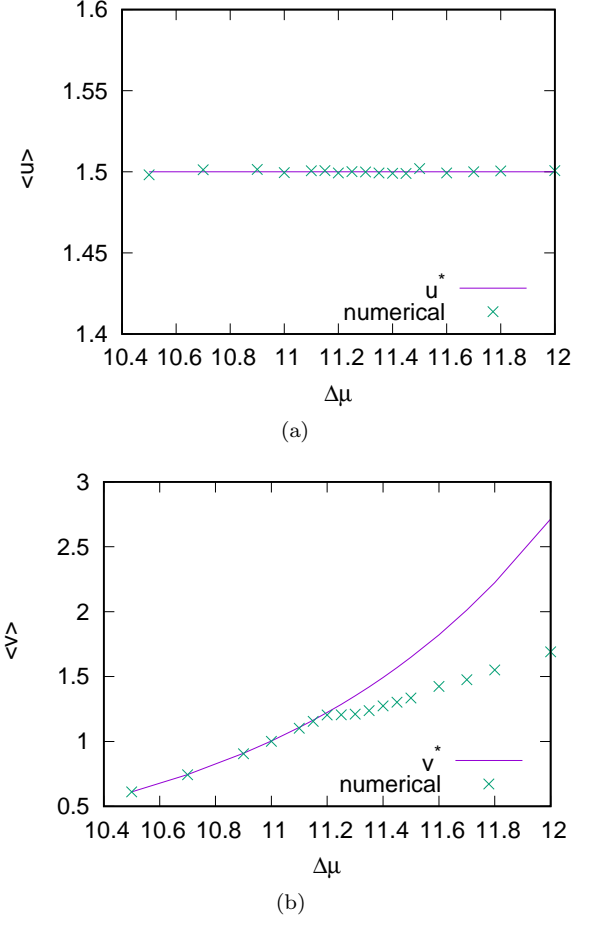


FIG. 2. (Color online) Average densities as functions of the thermodynamic force $\Delta\mu$. The values for the homogeneous fixed point solution in Eq. (7) are represented by the full magenta line.

above equation is

$$u^* = \frac{a_1}{a_2} \quad v^* = \frac{b_1 u^* + c_2 (u^*)^3}{b_2 + c_1 (u^*)^2}. \quad (7)$$

The emergence of a Turing pattern is related to the stability of this homogeneous solution. Depending on the values of the parameters this solution may become unstable and an inhomogeneous one becomes stable. One of the conditions on the parameters for the formation of a pattern is that $\beta > \alpha$ [2].

As shown in Fig. 1, for large enough $\Delta\mu$, an oscillatory pattern is formed. Both chemical species oscillate, with the minimums of the concentration X at the same positions as the maximums of the concentration of Y , and vice versa. We can estimate the critical point $\Delta\mu_c \approx 11.1$ by analyzing the average densities

$$\langle u \rangle \equiv \langle L^{-1} \sum_{i=1}^L u_i \rangle \quad \langle v \rangle \equiv \langle L^{-1} \sum_{i=1}^L v_i \rangle, \quad (8)$$

where the brackets indicate an ensemble average. This result is shown in Fig. 2. Above the critical point the

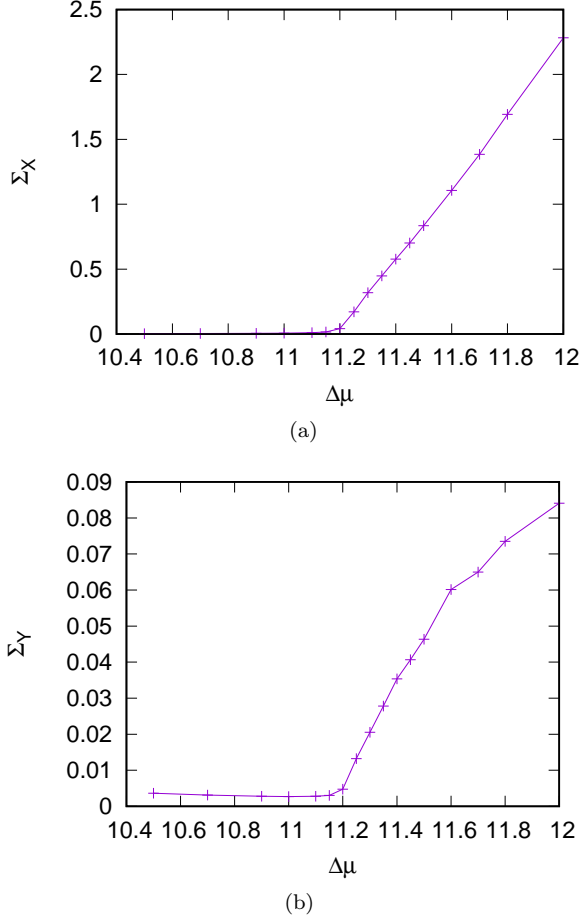


FIG. 3. (Color online) Relative standard deviations of the densities Σ_X and Σ_Y as functions of $\Delta\mu$. The crosses represent the values obtained from numerical simulations and the line is a guide to the eye.

average concentration of Y differs from the one obtained with the homogeneous fixed point.

Fluctuations of the densities are quantified by

$$\Sigma_X = \frac{\langle (u - \langle u \rangle)^2 \rangle}{\langle u \rangle^2} \quad \Sigma_Y = \frac{\langle (v - \langle v \rangle)^2 \rangle}{\langle v \rangle^2}. \quad (9)$$

As shown in Fig. 3, these quantities increase sharply above the critical point. These fluctuations do not quantify the precision of the pattern but rather their increase with $\Delta\mu$ is simply related to the fact that the square of the deviation from the mean is typically much larger for a periodic profile than for a flat profile. In the next two sections we analyze the relation between precision and dissipation of a pattern in the regime $\Delta\mu > \Delta\mu_c$. Due to the large size of Σ_X in this regime, we cannot use the linear noise approximation.

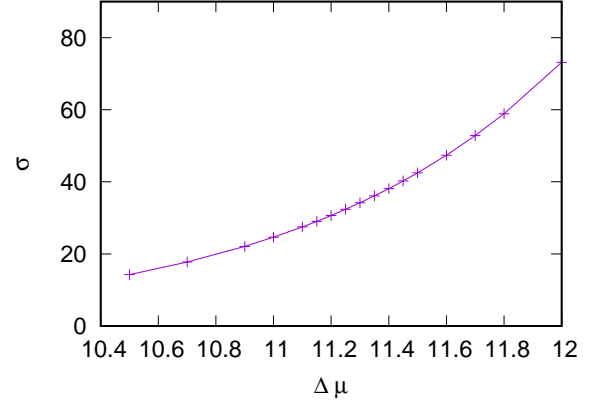


FIG. 4. (Color online) Average rate of entropy production σ as a function of $\Delta\mu$. The crosses represent the values obtained from numerical simulations and the line is a guide to the eye.

III. ENTROPY PRODUCTION

For a stochastic trajectory of duration T , the stochastic rate of consumption of the substrate S at cell i is given by $J_i = \theta_i/T$, where θ_i is a random variable that increases (decreases) by one whenever the chemical reaction $S + X_i \rightarrow Y_i + P$ ($Y_i + P \rightarrow S + X_i$) takes place. It is straightforward to evaluate J_i in a numerical simulation, by simply changing θ_i accordingly whenever these reactions take place. The average rate of entropy production per cell is

$$\sigma = \Delta\mu L^{-1} \sum_{i=1}^L \langle J_i \rangle. \quad (10)$$

In words, the rate of entropy production is the rate of substrate consumption multiplied by the chemical potential difference of transforming a substrate molecule S into a product molecule P . Diffusion reactions do not show up explicitly in this expression for σ since the ratio of a diffusion transition and its reverse is one [33]. However, σ does depend on diffusion rates since $\langle J_i \rangle$ depends on these rates.

In Fig. 4 we plot σ as a function of $\Delta\mu$. We observe that the rate of entropy production is an increasing function of $\Delta\mu$, the larger the thermodynamic force the larger the thermodynamic cost. In the next section we analyze the precision of the pattern as a function of $\Delta\mu$. Since the thermodynamic cost quantified by σ is an increasing function of $\Delta\mu$, we refer to increasing (decreasing) $\Delta\mu$ as increasing (decreasing) the thermodynamic cost.

Interestingly, there is a spatial profile of the entropy production if we consider a single stochastic trajectory, as shown in Fig. 5. The quantity $\sigma_i = \Delta\mu J_i$, which is the rate of entropy production at site i , displays spatial oscillations. The peaks of σ_i coincide with the peaks of u_i , since a larger density of X molecules increases the likelihood of the chemical reaction $S + X_i \rightarrow Y_i + P$.

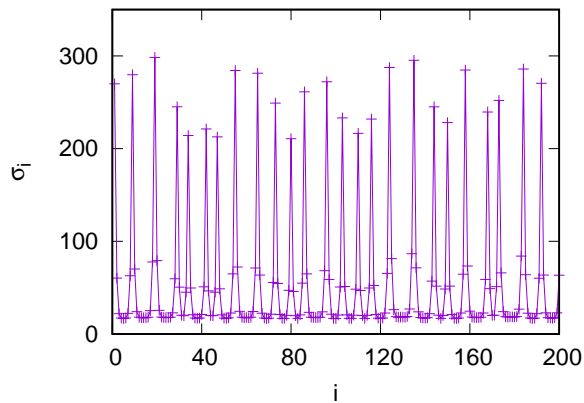


FIG. 5. (Color online) Spatial profile of the stochastic rate of entropy production σ_i for $\Delta\mu = 11.8$.

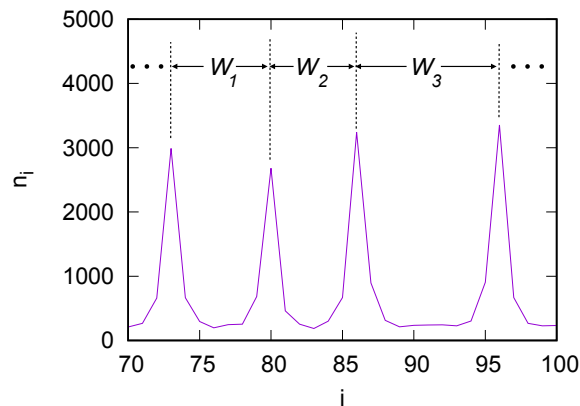


FIG. 6. (Color online) Illustration of the variable w , which is the distance between two peaks. For a given profile the variable w is the sum of the distance between neighboring peaks divided by the total number of peaks. These distances are illustrated as w_1 , w_2 and w_3 in the figure.

The critical behavior of the average rate of entropy production has been investigated in several models [25, 39–43]. We cannot identify any non-analytical behavior of rate of entropy production σ or its first derivative with respect to $\Delta\mu$ within our numerics, which does not discard non-analytical behavior of higher order derivatives.

IV. OPTIMAL PRECISION

A. The positive effect of fluctuations

The pattern formed in a stochastic reaction-diffusion model fluctuates, in contrast to a pattern that is formed in the deterministic case. We now analyze the precision of a stochastic pattern.

In order to quantify the precision of the pattern we consider the distance between two peaks w , which is il-

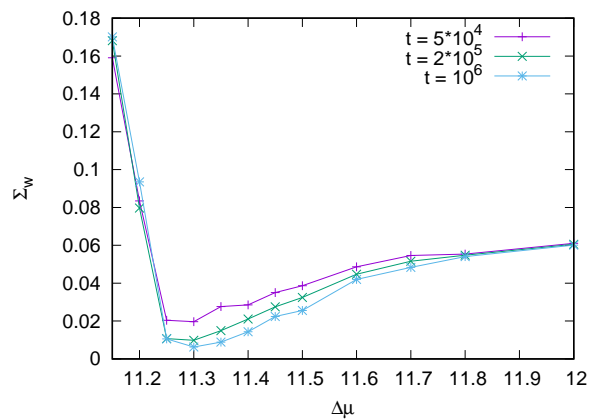


FIG. 7. (Color online) Relation between precision of a pattern and thermodynamic cost. The relative standard deviation Σ_w as a function $\Delta\mu$. The lines are guides to the eye.

lustrated in Fig. 6. We analyze the profile of the X molecules since their peaks are more pronounced. Fluctuations of w are quantified by

$$\Sigma_w = \frac{\langle w^2 \rangle - \langle w \rangle^2}{\langle w \rangle^2}. \quad (11)$$

The fluctuations in the distance between two peaks has been used to quantify the precision of temporal biochemical oscillations [23].

In Fig. 7 we plot Σ_w as a function of $\Delta\mu$. For the time $t = 10^6$, this function seems to be close to saturation. Surprisingly, this function is not monotonically decreasing. There is an optimal value $\Delta\mu \approx 11.3$ for which Σ_w is minimum. Hence, increasing the thermodynamic cost beyond this optimal value leads to a profile that is less precise.

A possible explanation for this result is as follows. If we watch a movie of the time evolution of a profile, we see that for larger $\Delta\mu$ the profile displays less pronounced fluctuations in the peak position, which remain static for longer periods of time for larger $\Delta\mu$. Hence, these fluctuations get less pronounced with an increase in thermodynamic cost. However, they can also be beneficial for the precision quantified by Σ_w . The pattern that is formed after some transient from the flat initial conditions depends on the particular stochastic trajectory. This pattern is different from the “correct” deterministic pattern. For large $\Delta\mu$ the system gets stuck in this pattern formed after the initial transient, and fluctuations cannot alter the position of the peaks.

Fluctuations of the peak positions have then two competing effects on the precision of the pattern. The straightforward effect is that too much fluctuations destroy the precision of the pattern. The surprising effect is that fluctuations that are too small do not allow the system to “correct” a sort of metastable pattern that is formed after the initial transient. The competition between these two effects leads to the optimal precision in

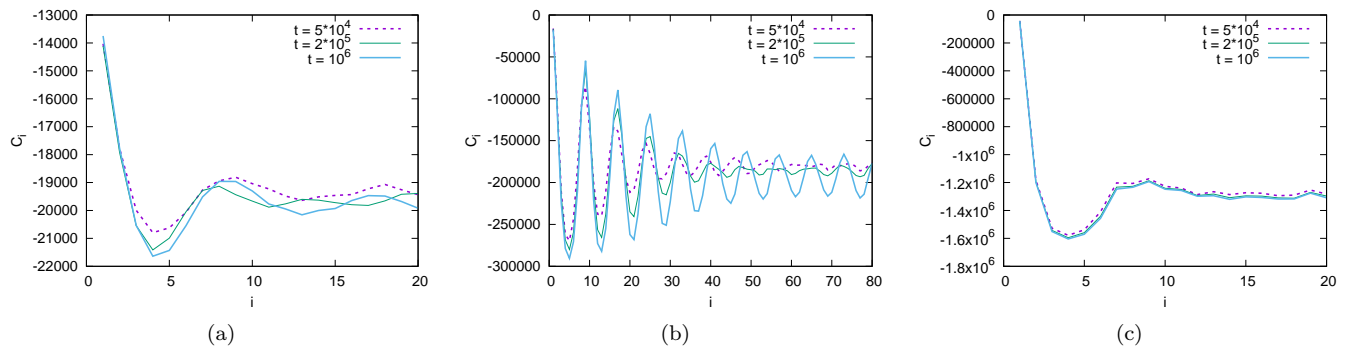


FIG. 8. (Color online) Spatial correlation C_i for (a) $\Delta\mu = 11$, (b) $\Delta\mu = 11.3$ and, (c) $\Delta\mu = 12$.

Fig. 7.

The relation between precision and dissipation depends on the particular choice of how the transition rates depend on parameters such as $\Delta\mu$. While several models for temporal biochemical oscillations do display a behavior for which precision improves with an increase in thermodynamic cost [23], examples for which precision of some kind is optimal at some intermediate thermodynamic cost do exist [24, 25, 32, 44]. The result for this particular model that could be general, independent of the way transition rates depend on parameters, is that fluctuations also have a positive effect on the precision of a pattern in a finite system within finite time.

B. Spatial correlation function

The random variable w is hard to formally define with an equation (see [28] for a discussion about this random variable concerning temporal oscillations). If we were to consider lower values of $\Delta\mu$, which are closer to the value of $\Delta\mu$ for which a pattern is first formed, it would be hard to differentiate between a peak and a fluctuation. A well defined observable that quantifies the precision of the pattern is the spatial correlation function

$$C_i = \sum_{j=1}^L (\langle n_j n_{j+i} \rangle - \langle n_j n_j \rangle). \quad (12)$$

As shown in Fig. 8, this quantity displays oscillations that decay exponentially in space. The number of coherent spatial oscillations, which is the correlation length divided by the average distance between two peaks, quantifies the precision of a pattern. This number of coherent oscillations is also used to quantify the precision of temporal oscillations [23, 24]. It is hard to get an exact value for this quantity and plot it as a function of $\Delta\mu$ within our numerics. However, we do find clear evidence of our main result that precision is optimal for an intermediate

thermodynamic cost. This evidence is shown in Fig. 8, where the spatial oscillations in the correlation function are more robust for an intermediate value of $\Delta\mu$.

V. CONCLUSION

We have analyzed the relation between precision of a spatial pattern and dissipation in a model that displays spontaneous pattern formation, the one dimensional Brusselator. A main result is that fluctuations of the peak positions can also have a positive effect on the precision of the pattern, as they correct the “metastable” pattern that is formed after an initial transient of the stochastic dynamics. Such fluctuations also have the standard effect of decreasing the precision of the pattern. These competing effects leads to the result that the precision of the spatial pattern is optimal for an intermediate thermodynamic cost.

Concerning future work we have considered a model with spatial oscillations and no temporal oscillations. It would be interesting to analyze the relation between temporal and spatial oscillations within models that display both oscillations, which are known as chemical waves [45]. Furthermore, the investigation of the effect of dimensions, reaction scheme, system size, and boundary conditions on the relation between precision and thermodynamic cost of a Turing pattern will elucidate the degree of generality of the results found within the present model.

From a broader perspective, two universal results within stochastic thermodynamics concerning the relation between precision and thermodynamics cost are the thermodynamic uncertainty relation [19] and the bound on the number of coherent temporal oscillations obtained in [24]. The question whether a general relation between spatial precision of some kind and thermodynamic cost exists remains an open one. Finally, it is an intriguing perspective to ask whether biological systems operate close to the optimal value of the thermodynamic cost.

-
- [1] A. M. Turing, Phil. Trans. R. Soc. Lond. B **237**, 37 (1952).
- [2] J. D. Murray, *Mathematical Biology II: Spatial Models and Biomathematical Applications* (Springer-Verlag New York, 2003).
- [3] S. Kondo and T. Miura, Science **329**, 1616 (2010).
- [4] P. C. Bressloff, *Stochastic Processes in Cell Biology* (Springer, 2014).
- [5] C. A. Lugo and A. J. McKane, Phys. Rev. E **78**, 051911 (2008).
- [6] T. Butler and N. Goldenfeld, Phys. Rev. E **80**, 030902 (2009).
- [7] T. Biancalani, D. Fanelli, and F. Di Patti, Phys. Rev. E **81**, 046215 (2010).
- [8] T. Butler and N. Goldenfeld, Phys. Rev. E **84**, 011112 (2011).
- [9] T. E. Woolley, R. E. Baker, E. A. Gaffney, and P. K. Maini, Phys. Rev. E **84**, 046216 (2011).
- [10] L. J. Schumacher, T. E. Woolley, and R. E. Baker, Phys. Rev. E **87**, 042719 (2013).
- [11] T. Biancalani, F. Jafarpour, and N. Goldenfeld, Phys. Rev. Lett. **118**, 018101 (2017).
- [12] F. D. Patti, L. Lavacchi, R. Arbel-Goren, L. Schein-Lubomirsky, D. Fanelli, and J. Stavans, PLoS Biol **16**, e2004877 (2018).
- [13] D. Karig, K. M. Martini, T. Lu, N. A. DeLateur, N. Goldenfeld, and R. Weiss, Proc. Natl. Acad. Sci. U.S.A. **115**, 6572 (2018).
- [14] H. Qian, Annu. Rev. Phys. Chem. **58**, 113 (2007).
- [15] G. Lan, P. Sartori, S. Neumann, V. Sourjik, and Y. Tu, Nature Phys. **8**, 422 (2012).
- [16] P. Mehta and D. J. Schwab, Proc. Natl. Acad. Sci. U.S.A. **109**, 17978 (2012).
- [17] C. C. Govern and P. R. ten Wolde, Phys. Rev. Lett. **113**, 258102 (2014).
- [18] A. C. Barato, D. Hartich, and U. Seifert, New J. Phys. **16**, 103024 (2014).
- [19] A. C. Barato and U. Seifert, Phys. Rev. Lett. **114**, 158101 (2015).
- [20] T. McGrath, N. S. Jones, P. R. ten Wolde, and T. E. Ouldridge, Phys. Rev. Lett. **118**, 028101 (2017).
- [21] D. Chiuchiu, Y. Tu, and S. Pigolotti, Phys. Rev. Lett. **123**, 038101 (2019).
- [22] H. Qian and M. Qian, Phys. Rev. Lett. **84**, 2271 (2000).
- [23] Y. Cao, H. Wang, Q. Ouyang, and Y. Tu, Nature Phys. **11**, 772 (2015).
- [24] A. C. Barato and U. Seifert, Phys. Rev. E **95**, 062409 (2017).
- [25] B. Nguyen, U. Seifert, and A. C. Barato, J. Chem. Phys. **149**, 045101 (2018).
- [26] C. Fei, Y. Cao, Q. Ouyang, and Y. Tu, Nat. Commun. **9**, 1434 (2018).
- [27] H. Wierenga, P. R. ten Wolde, and N. B. Becker, Phys. Rev. E **97**, 042404 (2018).
- [28] R. Marsland, W. Cui, and J. M. Horowitz, J. R. Soc. Interface **16**, 20190098 (2019).
- [29] D. Zhang, Y. Cao, Q. Ouyang, and Y. Tu, Nat. Phys. **16**, 95 (2020).
- [30] C. del Junco and S. Vaikuntanathan, Phys. Rev. E **101**, 012410 (2020).
- [31] C. del Junco and S. Vaikuntanathan, J. Chem. Phys. **152**, 055101 (2020), <https://doi.org/10.1063/1.5143259>.
- [32] J. H. Fritz, B. Nguyen, and U. Seifert, arXiv:2003.02148 (2020).
- [33] U. Seifert, Rep. Prog. Phys. **75**, 126001 (2012).
- [34] G. Falasco, R. Rao, and M. Esposito, Phys. Rev. Lett. **121**, 108301 (2018).
- [35] A. J. McKane, T. Biancalani, and T. Rogers, Bull Math Biol **76**, 895 (2014).
- [36] N. G. van Kampen, *Stochastic Processes in Physics and Chemistry* (North-Holland, Amsterdam, 1981).
- [37] V. Klika, M. Kozák, and E. A. Gaffney, SIAM J. Appl. Math. **78**, 2298 (2018).
- [38] D. T. Gillespie, J. Phys. Chem. **81**, 2340 (1977).
- [39] L. Crochik and T. Tomé, Phys. Rev. E **72**, 057103 (2005).
- [40] M. J. de Oliveira, J. Stat. Mech. , P12012 (2011).
- [41] T. Tomé and M. J. de Oliveira, Phys. Rev. Lett. **108**, 020601 (2012).
- [42] A. C. Barato and H. Hinrichsen, J. Phys. A Math. Theor. **45**, 115005 (2012).
- [43] Y. Zhang and A. C. Barato, J. Stat. Mech. **2016**, 113207 (2016).
- [44] M. Baiesi and C. Maes, J. Phys. Comm. **2**, 045017 (2018).
- [45] F. Avanzini, G. Falasco, and M. Esposito, J. Chem. Phys. **151**, 234103 (2019).